STATISTICAL ANALYSIS AND INTERCOMPARISON OF GLOBAL ERS-1 SAR WAVE MODE SPECTRAL RETRIEVALS USING WAM MODEL AND BUOY DATA

P. Heimbach, S. Hasselmann, K. Hasselmann and M. Toporek

Max-Planck-Institut für Meteorologie, Bundesstraße 55, D-20146 Hamburg, Germany
Phon: + 49 / 40 / 4 11 73 - 3 77, Facs: + 49 / 40 / 4 11 73 - 2 98
E-mail: heimbach@dkrz.de

Abstract

A global statistical intercomparison was carried out for the period January 1993 to December 1995 between wave spectra retrieved from ERS-1 SAR Wave Mode (SWM) data using an inversion algorithm of the closed nonlinear wave-to-SAR spectral mapping relation and wave spectra computed with the wave model WAM. A combined quality analysis of the satellite data and a performance analysis of the retrieval algorithm was performed. The assessment yielded about 75 percent successful retrievals. The histogram of pattern correlation between best estimate and observed SAR spectra is sharply peaked at 0.9. The retrieval was repeated using 1,000 collocated buoy spectra as first guess. Both retrievals agreed very closely in terms of the mean spectral parameters, confirming that the retrieval is independent of the first guess. The azimuthal cut-off wavenumber, a measure of the rms orbital velocity, was investigated. Despite the limited resolution in azimuth due to this cut-off, about 75 % of the swell is explicitly resolved by the SAR, proving its general ability to detect a significant part of the ocean wave field. Comparing the cut-off wavenumber to the wind speed no simple relationship between both quantities could be found, as additional effects such as wave age or fetch were not taken into account.

Keywords: ocean waves; ERS-1 SAR Wave Mode; spectral retrieval algorithm; WAM model; 2d buoy spectra; global statistics; windsea and swell partitioning; azimuthal cut-off wavenumber.

1. INTRODUCTION

One of the major goals for the first European Remote Sensing Satellite ERS-1, launched on 17 July 1991, was to obtain global wind and wave data in near real time for wave research and operational wave forecasting. A particularly useful feature of the ERS-1 microwave instrument is the Synthetic Aperture Radar (SAR) intermittent imaging mode (so-called "wave mode"). This provides global two-dimensional wave spectral image data derived from 5 $\times$ 10 km imagettes observed every 200 km along the satellite track (for a detailed description see Appendix A1 of [*Heimbach et al.*, 1997] and [*Brooker*, 1995]). The image spectra can be converted to wave spectral data, which can then be used to validate global wave models and improve wave forecast through wave data assimilation (see [*Komen et al.*, 1994]). On 21 April 1995, ERS-2 was launched replacing ERS-1 in providing near real time global SAR Wave Mode (SWM) data. It is hoped that the continuity and operational application of global SAR wave data will be ensured in the future through the launch of ENVISAT planned for 1999, which deploys an Advanced SAR (ASAR).

The retrieval of ocean wave spectra from Wave Mode imagette spectra is not a simple exercise. The SAR imaging mechanism is strongly nonlinear because

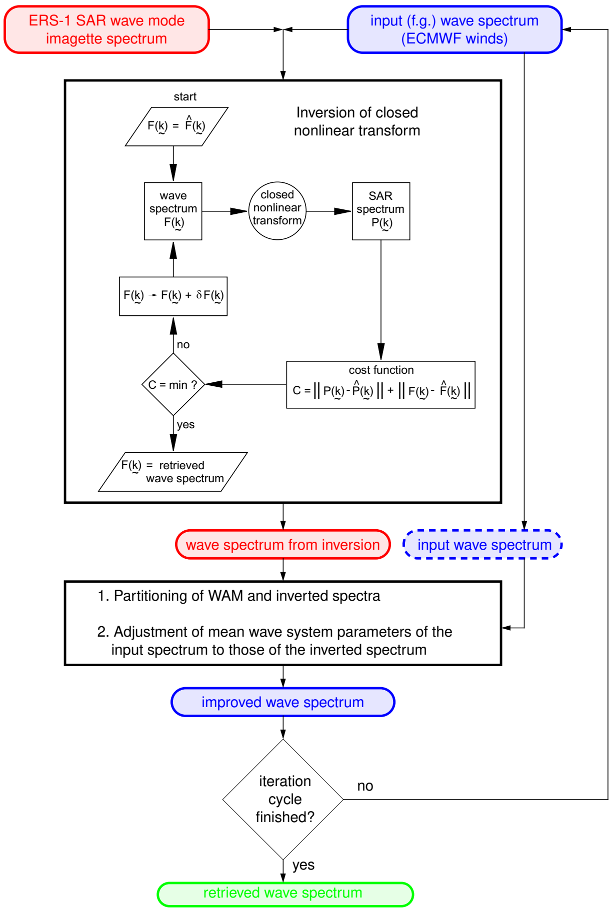

Figure 1: Flow chart for the retrieval algorithm of wave spectra from ERS-1 SWM spectra.

of the distortions induced by the wave orbital motions, the "velocity bunching mechanism" (cf. the MARSEN review in *Hasselmann et al.* [1985]). This leads, among other effects, to image smearing and to a loss of information beyond the so-called azimuthal cut-off wavenumber, corresponding typically to wavelengths shorter than about 100 – 200 m in the satellite flight direction. In addition, ocean wave spectra from satellite SAR images suffer from a basic 180° frozen-image ambiguity. Nevertheless, even with these limitations, *Hasselmann and Hasselmann*, [1991], (referred to in the following as [HH]) were able to develop an efficient inversion algorithm enabling a retrieval of ocean wave spectra from SAR imagette spectra within the computational constraints of real-time operational applications (see also [*Krogstad et al.*, 1994]). An important feature of SAR spectral retrieval algorithms is the availability of an internal calibration of the retrieved wave spectra, without reference to the SAR instrument calibration or measurements of the absolute backscattering cross section. This is achieved by calibrating against the clutter or speckle background noise spectrum that is superimposed on and therefore measured simultaneously with the wave modulation spectrum. However, the original method of *Alpers and Hasselmann*, [1982] for standard energy-averaged multi-look images needed to be modified to allow for the amplitude averaging employed in the ERS-1 SAR Wave Mode multi-look processing [*Brüning et al.*, 1994].

An essential prerequisite for the construction of an operationally feasible inversion algorithm was the derivation by [HH] of a closed nonlinear integral transform describing the mapping of ocean wave spectra into SAR spectra. It contains an exponential factor $\exp[-k_x^2\xi^2]$ that describes the fall-off of the image spectrum beyond an azimuthal cut-off wavenumber k_x, where $\xi = v \cdot R/U$ is the rms azimuthal displacement, given by the product of the rms orbital (range) velocity v and the range-to-platform velocity ratio $\beta = R/U$. To overcome the 180° directional ambiguity and to supplement the missing SAR information beyond the azimuthal cut-off, a first guess wave spectrum is required as input to the retrieval algorithm. The imaging theory and nonlinear mapping relation have been verified in numerous studies (an overview is given in *Heimbach et al.* [1997], referred to in the following as [H3]). A first evaluation of this algorithm was performed by *Brüning et al.* [1994]. An improved algorithm has recently been proposed by [*Hasselmann et al.*,1996], (referred to in the following as [HBHH]). The input spectrum is now iteratively modified with the aid of a spectral partitioning scheme. Furthermore, the limitation imposed by the azimuthal smearing is partially overcome by

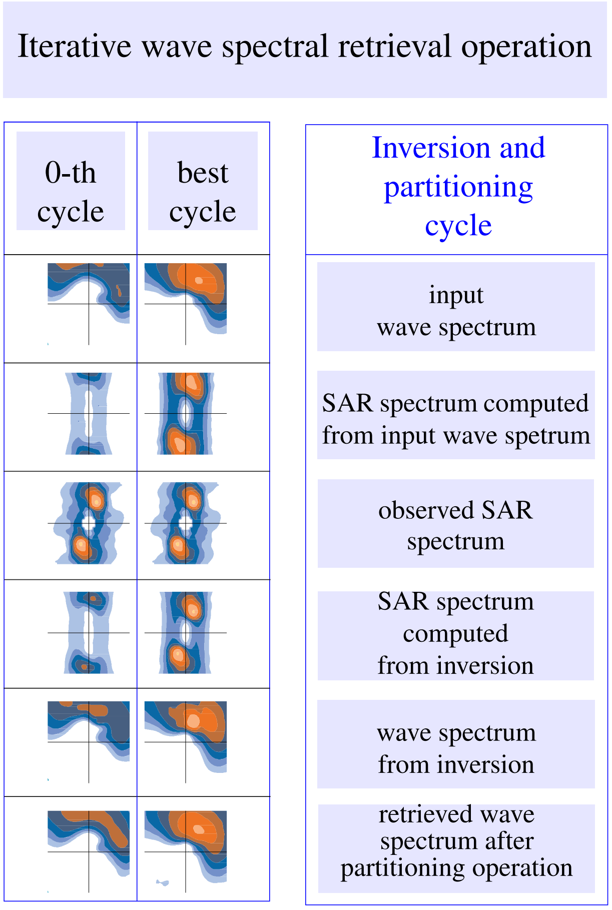

Figure 2: Example showing the intermediate steps of the retrieval of an ocean wave spectrum from an ERS-1 SWM imagette spectrum in the 2d wavenumber domain.

including an explicit penality term for errors in the azimuthal cut-off in the cost function. The retrieval algorithm of [HBHH] has been used in this study.

The WAM model plays an important role in our analysis (for a description of the present cycle 4 see [*WAMDI Group*, 1988] and [*Komen et al.*, 1994]). The model spectra were computed with the operational wave forecast model WAM cycle 4 at the European Centre for Medium-Range Weather Forecasts (ECMWF) every 6 hours on a global 3° × 3° (since July 1994: 1.5° × 1.5°) latitude-longitude grid. As wind forcing we used the ECMWF analyzed wind field at 10m height. The initial and analysed WAM spectra nearest to the SWM footprint along the ERS-1 and ERS-2 satellite orbits are stored and archieved at ECMWF yielding by now a six year archive of model spectra collocated to SWM data, available e.g. for retrieval purposes

The WAM spectra were used to provide the first guess for the wave spectral retrievals, and we use the WAM model predictions again in intercomparing the modelled and retrieved wave spectra. This approach is not as circular as this may appear, since it has been demonstrated in [HBHH] and will again be investigated in section 5 that the improved retrieval algorithm used here, in which the first-guess input spectrum is iteratively modified, is insensitive to the initial input spectrum. The first guess information is used only to remove the 180° ambiguity and augment the retrieved spectrum beyond the azimuthal cut-off, so that asymptotically only the truly missing information is carried over from the first guess spectrum to the retrieval.

Alternative approaches to using WAM spectra as first guess have been proposed [*Mastenbroek and de Valk*, this issue]. They consist in using the wind vector derived from the ERS-1 scatterometer which is simultaneously operated together with the SWM (the same applies for ERS-2 and ENVISAT) from which a parametric windsea spectrum is derived. However, this method suffers from two drawbacks. First, the parametric spectrum has again to be considered as a model spectrum which yields in general a poorer first guess than the WAM model, second the 180° ambiguity of the swell cannot be resolved by this method. More promising techniques make use of the information on the wave propagation direction contained in successive multi-look or complex images (e.g. [*Engen and Johnsen*, 1995]). The provision of the real and imaginary part of the SAR cross-spectrum as fast delivery product is planned for ENVISATs ASAR enabling this technique to be operationally implemented.

2. RETRIEVAL ASSESSMENT

The 3 year set of ERS-1 SWM data between January 1993 and December 1995 comprises a total of some 1.2 million wave spectra with an average daily output

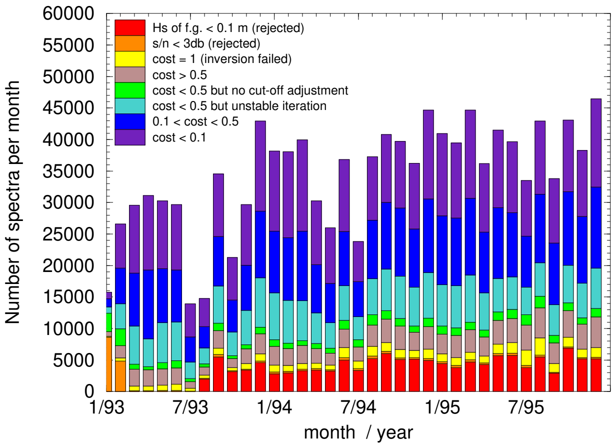

Figure 3: Assessment of the ERS-1 SWM data quality and the retrieval fidelity

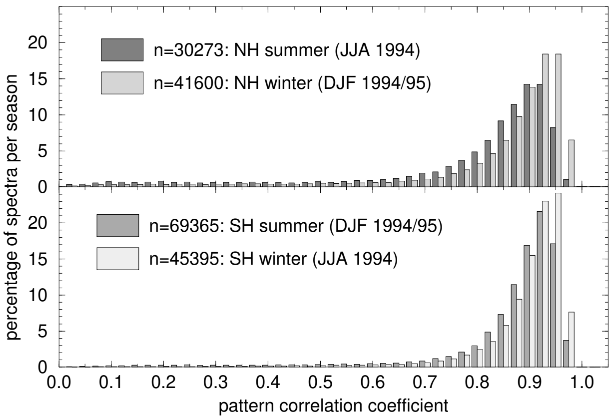

Figure 4: Distribution of pattern correlation between simulated and observed SAR spectra

of 1100 spectra. In this section the data quality and performance of the retrieval algorithm are discussed.

The retrieval process incorporated two quality tests: a data quality test for the input SWM data, and a reliability test for the retrieval. The input SWM data was rejected if the signal-to-noise ratio of the image spectrum (defined as the ratio of the spectral peak to the clutter noise background) was less than 3 db or if the first guess wave height was below 0.1 m. The retrieved spectra were discarded as unreliable if the cost function was not reduced to less than half of its initial value. Furthermore, all spectral information beyond 800 m wavelength was excluded. These frequently represent non-wave-like sea surface features like slicks, wind rows etc. (see [*Brüning et al.*, 1994]), while statistical analyses [*Heimbach et al.*, 1997] indicate that swell of extreme wavelengths beyond 600 to 700 m are rare.

Figure 3 shows that with the beginning of the quasi real-time distribution of the Fast Delivery Product (FDP) in February 1993 maximally 2 % of the data showed low signal-to-noise ratios. Another 10% of the data were rejected because the first guess wave height was too low ($H_s < 0.1$ m).

For roughly 85 % of the remaining data, the retrieval algorithm achieved an acceptable performance, with cost function reductions to less than 0.5 of the initial value, for one third a reduction factor of less than 0.1 was achieved. Spectra with a cost function reduction factor lower than 0.5 for which the azimuthal clutter cut-off adjustment or the convergence of the iterative inversion procedure was poor were nevertheless retained in the subsequent analysis, as their fidelity, (i.e. their ability to reproduce the observed SAR spectra), was generally still acceptable. The remaining 15% inversions for which the ratio of the final to initial cost could not be reduced below 0.5 generally exhibited relatively low pattern correlations between

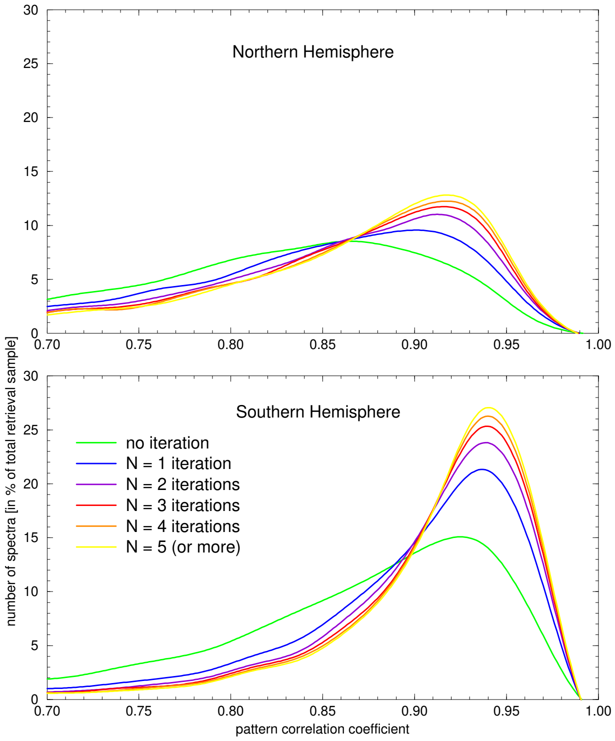

Figure 5: Distribution of pattern correlation in the Northern Hemisphere (top) and Southern Hemisphere (bottom). Each curve represents a retrieval experiment with a given number of maximum allowed iterations.

the simulated and observed SAR spectral and were discarded from the further analysis.

The retrieval fidelity is represented in Figure 4 in terms of the distributions of the pattern correlation coefficients for the simulated and observed SAR spectra for the summer 1994 and winter 1994/95 seasons in the Northern and Southern Hemisphere. All distributions show a rather narrow peak around 0.9, indicating that for the major part of the data successful retrievals of high fidelity were achieved. The winter distributions in both hemispheres appear to be peaked towards slightly higher correlations than the summer distributions, suggesting that the retrieval performance is generally higher for high sea states (as may be expected from the generally higher signal-to-noise ratios for higher sea states).

An assessment of the impact of the iteration of the input spectrum revealed that for about 92 % of the retrievals the iteration yielded an improvement, 75% showing a further improvement for more than one iteration (see [H3]). A retrieval exercise was performed seeking the minimum number of iterations which significantly improve the retrieval. Figure 5 depicts the distributions of the pattern correlation for a given maximum number of allowed iterations for the Northern and Southern Hemisphere during August 1995. The largest impact on the retrieval is found in performing the first iteration $M = 1$, suggesting that at least one iteration should be carried out. Two iterations may represent an acceptable trade-off of retrieval improvement against computing time, the additional improvements beyond $M = 2$ tending to be rather small. The impact of iteration is stronger in the Southern Hemisphere, i.e. for high sea states during winter season.

3. THE RMS ORBITAL VELOCITY

A basic limitation of SAR ocean wave imaging is the azimuthal cut-off of the image spectrum caused by the nonlinear velocity bunching mechanism [HH], [HBHH]. The cut-off normally lies within the wind-sea part of the spectrum and suppresses the direct spectral information provided by the SAR on short to moderate wavelength waves with significant components of propagation in the azimuthal direction. However, the azimuthal cut-off wavenumber also provides a direct measure of an important integral parameter of the wave field: the rms orbital velocity component in the range direction. This information is used in the retrieval algorithm to adjust the rms orbital velocity to reproduce the observed cut-off, thereby partially replacing the missing direct spectral information at high wavenumbers.

The retrieval algorithm was generally successful in adjusting the simulated to the observed cut-off parameter (see [H3]). To assess the amount of wind-sea and swell which can directly be resolved by the SAR we have computed the ratio of the observed azimuthal cut-off wavenumber to the wavenumber component in the azimuth direction for each swell system. Figure 6 depicts the resulting histograms of three samples for DJF 1995/96 for the Northern Hemisphere Extra-Tropics, the Tropics (between 25° N/S) and the Southern Hemisphere Extra-Tropics. The medians of the histograms are listed in Table 3. Also listed are the percentage of wave systems with ratios greater than 1, referring to waves which can be explicitly resolved by the SAR. The values clearly underline the ability of the ERS-1 SAR to detect a substantial amount of waves even for high R/v ratios.

A global map of the mean azimuthal cut-off wavelength λ_c for DJF 1995/96 is shown in Figure 7. High cut-off wavelengths corresponding to high rms orbital velocities are found, as expected, in the regions of high winds in mid-latitudes. In addition, pronounced fetch effects are seen. However, no simple relationship between λ_c and u_{10} was found. Deviations from the linear relationship proposed by *Chapron et al.*, [1995] which is expected to hold for

windsea / swell	median	percent of waves with ratio > 1
N-Hem.	0.65 / 1.4	34 / 72
Tropics	0.5 / 1.85	28 / 78
S-Hem.	0.65 / 1.5	35 / 74

Table 1: Characteristics of histograms of observed azimuthal cut-off wavenumber to wavenumber component in the azimuth direction.

fully developed waves, were found, varying strongly between the mid-latitudes and the Tropics. They reflect the dependency on additional quantities such as wave age (see also [*Kerbaol and Chapron*, this issue]).

4. STATISTICAL INTERCOMPARISON

Global and regional intercomparisons between the collocated spectral wave parameters retrieved from ERS-1 SWM spectra and computed with the WAM model were carried out for the 3 year period 1 January 1993 – 31 December 1995.

The time series of monthly mean significant wave height in different regions of the Atlantic, Pacific and Indian Ocean retrieved from ERS-1 SWM and

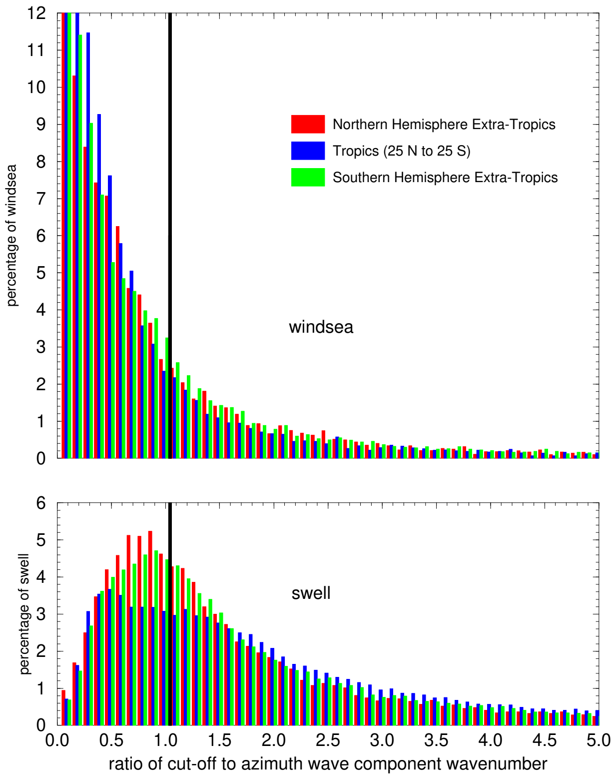

Figure 6: Histograms of windsea and swell systems with a given fraction of the observed azimuthal cut-off to the azimuth wavenumber component (step width: 0.1).

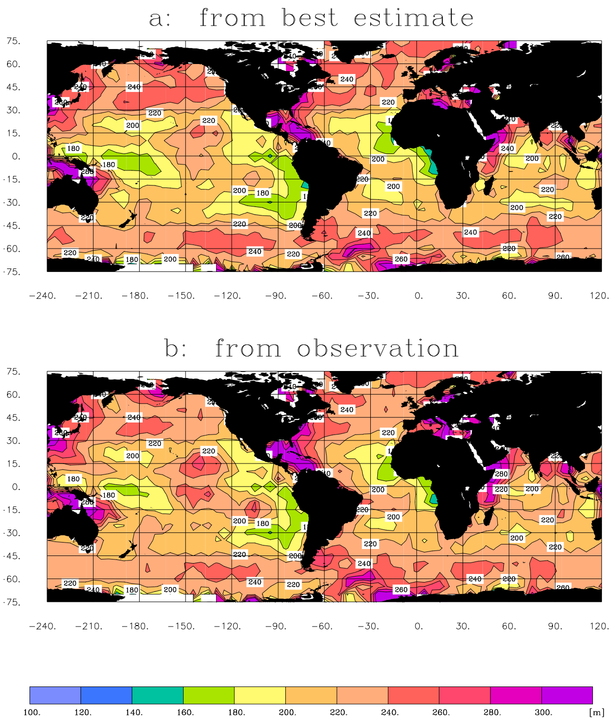

Figure 7: Global distribution of the seasonal mean azimuthal cut-off wavelength for DJF 1995/96.

computed by the WAM showed a satisfactory overall agreement [H3]. However, a small but systematic underestimation of H_s by the WAM relative to the ERS-1 SWM data was found.

For a more detailed intercomparison the modelled and retrieved wave spectra were partitioned into windsea and swell systems as defined in [HBHH]. The time series of the monthly mean windsea H_{wi} and swell H_{sw} wave heights for the modelled and retrieved wave spectra in different basins of the Atlantic, Pacific and Indian Ocean revealed small systematic deviations [H3]. Whereas the WAM windsea tends to be slightly overpredicted by about 10 % relative to the retrieved data, with larger relative deviations for high sea states corresponding to winter conditions, the swell wave heights are systematically underestimated by about 20 to 30 %. The different features of the windsea and swell biases cannot be explained simply by a dependence on wave height, but must be attributed to the different spectral and dynamical properties of windsea and swell. We have considered three possible causes for the differences:

1. Results from data assimilation exercises suggest that in certain areas of the Atlantic and Pacific the ECMWF analysed wind fields produce too strong winds and thus too strong windseas (see [*Bauer et al.*, 1996], [*Hasselmann et al.*, 1997] and references in [*Bauer et al.*, 1997]). However, if this were the only error, an overestimation of the windsea would

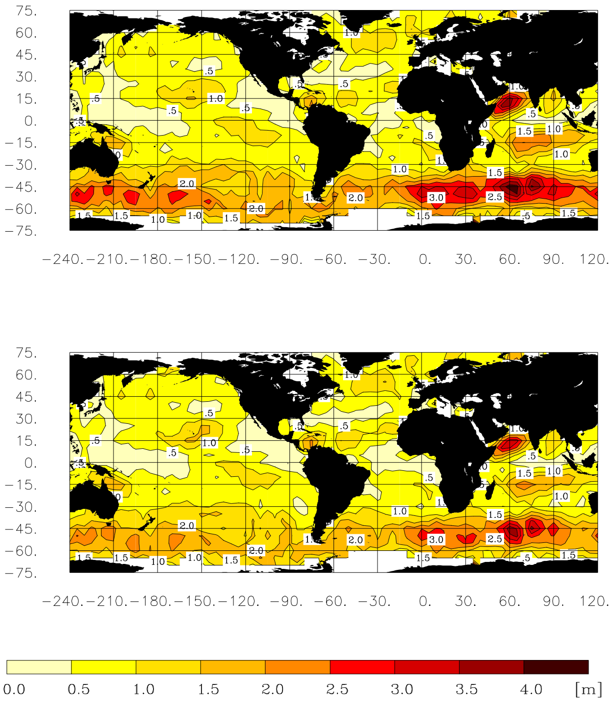

Figure 8: Global distribution of WAM (top) and SWM (bottom) seasonal mean windsea wave heights during JJA 1994.

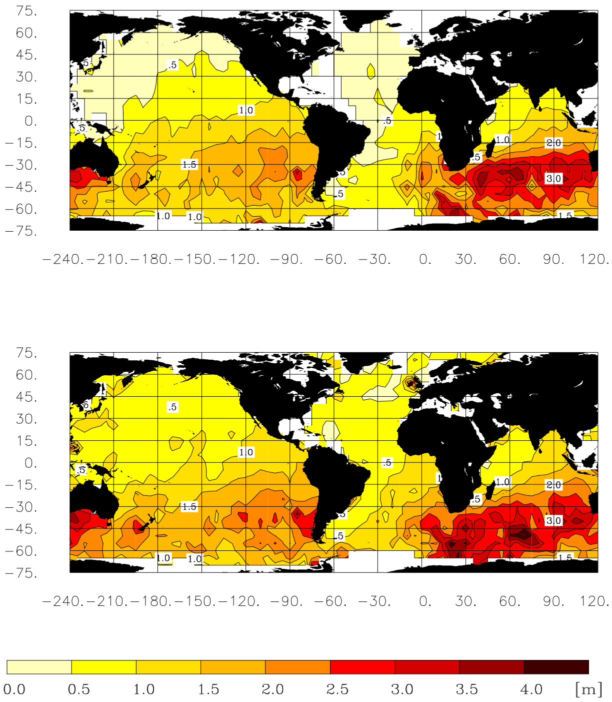

Figure 9: Same as Figure 8 but for individual swell components of largest wavelength exceeding 250m.

necessarily lead also to an overestimation of the swell emerging from the storm, which is not found.

2. The combination of an overestimation of the windsea together with an underestimation of swell suggests a possible error in the balance between windsea and swell dissipation.

3. The transition regime between windsea and swell in the area close to but outside the immediate wind generation region, plays a critical role in determining the ratio of windsea to swell energy. It is conceivable that the simplified discrete interaction parametrization of the nonlinear energy transfer is inadequate for a proper representation of this process.

Numerical errors associated with the propagation scheme employed in the WAM model ([*WAMDI Group*, 1988]) can be excluded because the propagation scheme is energy conserving. Furthermore, an erroneous impact of the frequency on the modulation transfer functions is improbable as no dependency of the windsea and swell biasses on the wave frequency was observed.

We regard the second candidate of a too strong damping for low frequency swell as the most likely explanation for the negative swell bias (for a more detailed discussion see [H3]).

Another possible source of error is indirect errors introduced by altimeter data. Since August 1993 ERS-1 altimeter wave height data have been assimilated by ECMWF into the operational WAM model using an optimal interpolation scheme, thereby influencing the first guess wave field through the analysis six hours earlier. However, an investigation of altimeter wave heights suggests that the impact on the first guess data available for the present study is probably rather limited (see the discussion in [H3]). We are therefore reasonably confident that, although our model data are undoubtedly affected by the assimilation of altimeter data, the dynamical aspects are at least still apparent in the data set.

Further investigations were performed looking at regionally stratified collocated WAM and SAR wave data subdivided again into windsea and swell as a function of season. As examples we show here the global distributions of all collocated WAM and SAR wave data for austral winter JJA 1994 (Figure 8a,b for windsea and 9a,b for swell). The plots confirm the previous findings of a generally overestimated windsea and underestimated swell by the WAM relative to the SWM retrievals. Whereas the windsea maps reflect the seasonal local properties of the atmospheric circulation (see e.g. the local effect of summer monsoon in the Arabian Sea) the non-local patterns for swell are seen to be very similar to the maps of mean swell wavelengths (see [H3]). One can thereby readily identify the main areas into which the long wavelength swell is radiated from the mid-latitude source regions.

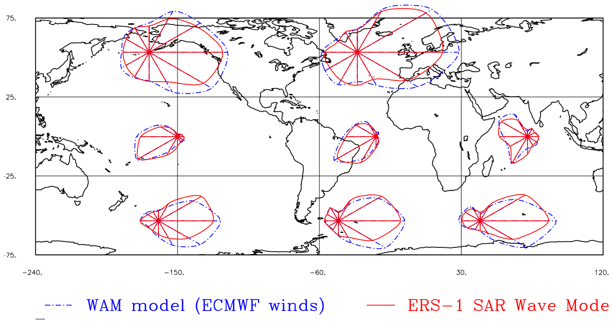

Figure 10: Seasonal mean directional windsea wave height distribution during DJF 1993/94 in several regions of the world oceans.

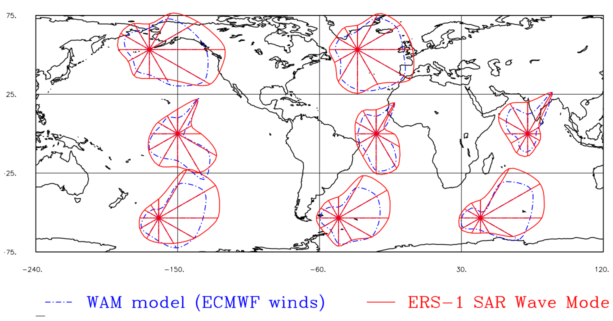

Figure 11: Same as Figure 10 but for swell.

As another example illustrating the detailed spectral, directional and regional information contained in the ERS-1 SWM data, we present in Figures 10 and 11 the retrieved and modelled "directional wave roses" representing the energy-weighted distributions of the wave propagation directions for windsea and swell, respectively, during JJA 1994 for different regions. The wave roses were computed as the square root of the mean energy for each 30° angular sector (for details see [H3]). Differences in the local vs. non-local character of windsea and swell, respectively, can again be noticed, e.g. swell from the Northern Hemisphere propagating into the Southern Hemisphere.

5. ERS-1 SWM vs. BUOY INTERCOMPARISON

Besides assessing the data quality and retrieval performance several validation exercises have been carried out. Significant wave heights retrieved from SWM data were compared with altimeter-derived H_s from the TOPEX and the ERS-1 satellites (for details see [*Bauer and Heimbach*, 1997] and [*Heimbach et al.*, this issue]). Here, we present an intercomparison between ERS-1 SWM spectral retrievals and buoy spectra collocated during 1993 (further collocations for 1994 and 1995 are in progress). The buoy data were obtained from heave, pitch and roll buoys operated by the National Oceanographic and Atmospheric Administration (NOAA). Except one buoy off Hawaii, all buoys are located near the American continent, sufficiently off the shore to exclude orographic or coastal effects. Four buoys are situated in the North Pacific, four buoys in the North Atlantic. The high resolution buoy spectra (40 linear frequency intervalls, 72 angular sectors of 5°) were interpolated to the WAM grid to match the model data. In total 1652 buoy spectra were collocated, however allowing a spatial window of 600 km distance. While this is sufficient for the present sensitivity study, a rigorous validation would restrict the distance to about 150 km. The ongoing work to collocate the 1994 and 1995 data will provide a larger data set to establish a sample with strict collocation criteria for direct validation and improved statistical significance.

Complementary to the retrieval of ocean wave spectra from SWM data using WAM spectra as first guess, a second retrieval exercise was carried out using buoy data as input. A symmetric regression between both retrievals was performed, taking into account those retrieval pairs only which jointly fulfill the retrieval quality criteria described in section 2 (notation: $y = b_{sym} \cdot x$, with mean $< . >$, bias $\Delta = <x> - <y>$, symmetric slope b_{sym} and correlation coefficient r). This yielded a subsample of roughly 1000 spectra. The regression for the significant wave heights, swell wave heights, mean total frequency and swell frequency reveal good agreement between both retrievals (see Table 5 for parameters of the total spectrum). This again confirms that the retrieval algorithm is largely independent of the first guess input spectrum. Larger differences only appear in comparing the windsea retrievals. This can

	WAM W-ret.	Buoy B-ret.	WAM Buoy	W-ret. B-ret.
	significant wave height			
$<x>$ / m	2.53	2.16	2.53	2.57
$<y>$ / m	2.57	2.57	2.16	2.57
Δ / m	-0.04	-0.41	0.37	0.00
b_{sym}	1.02	1.16	0.89	1.02
r	0.73	0.71	0.72	0.82
	mean frequency			
$<x>$ / Hz	0.108	0.118	0.108	0.105
$<y>$ / Hz	0.105	0.104	0.118	0.104
Δ / Hz	0.003	0.014	-0.010	0.001
b_{sym}	0.964	0.871	1.097	0.991
r	0.688	0.494	0.581	0.760

Table 2: Statistical parameters of symmetric regression for total spectra.

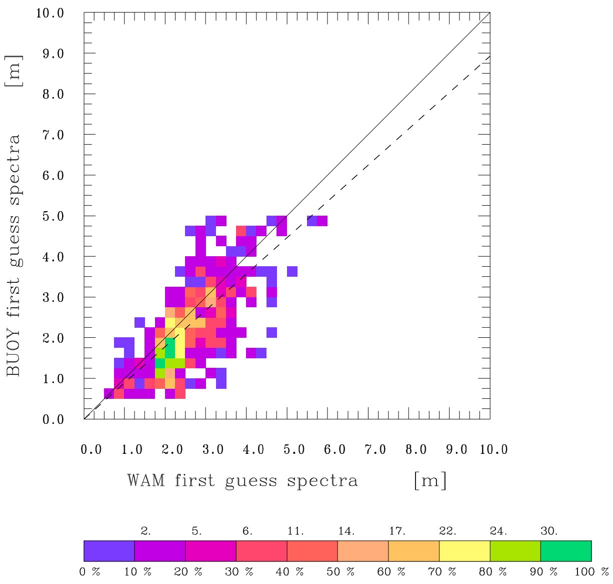

Figure 12: Regression of H_s between WAM and buoy.

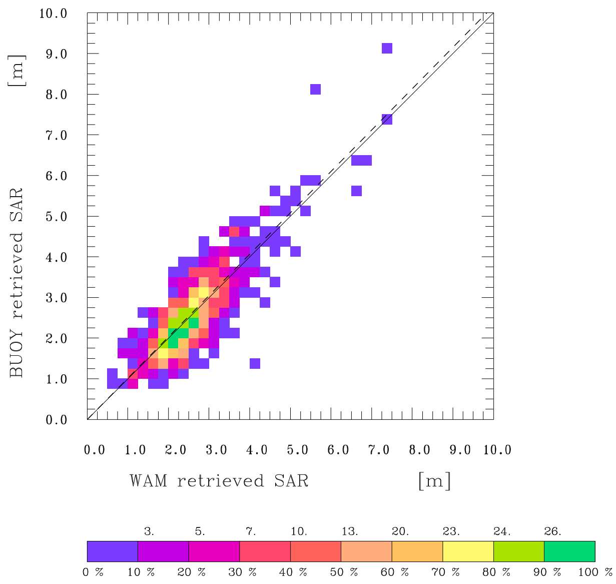

Figure 13: Regression of H_s between ERS-1 SWM retrievals using WAM and buoy as first guess input.

be expected as the windsea spectrum also contains information which is asymptotically missing in the SAR image spectrum.

A direct comparison between buoy and WAM data reveals in general significant differences in terms of the mean spectral parameters. This can partly be explained by the large allowed collocation distance. The same applies for the comparison between buoy and buoy-input retrieved data. Furthermore, it should be noted that high sea states are extremely rare in the data sample. Therefore, no conclusions can be drawn yet with respect to direct validation of SWM retrievals using buoy spectra. However, validating SWM-retrieved significant wave heights using altimeter data showed a good agreement between the data sets considered [*Heimbach et al.*, this issue].

6. CONCLUSIONS

An assessment was carried out of the ERS-1 SWM data quality and the performance of the wave spectral retrieval algorithm of [HBHH] over the three year period January 1993 – December 1995. Furthermore, various intercomparisons were performed between ERS-1 SWM spectral retrievals and collocated WAM model data as well as collocated buoy measurements. This study, together with the work by *Heimbach et al.*, [this issue] underlines the importance of achieving a synthetic view from all available data sources, i.e. model, remotely sensed and in-situ data, be they integral or spectral in nature, to adequately interpret the retrieval and the model results. From the present study the following conclusions can be drawn:

1. Only few SWM spectra had to be rejected due to low quality. The performance analysis revealed 75 % of the FDP data to be successfully retrieved. The distribution of the pattern correlation between the SAR spectrum simulated from the retrieved wave spectrum and the observed SAR spectrum is peaked at 0.9. Iteratively improving the input spectrum was found to be beneficial, particularly in estimating the high wavenumber spectral energy content and in further reducing the dependnecy of the retrieval on its first guess.
2. Despite the fact that SAR imaging is highly nonlinear for ERS-1 leading to a fall-off of the spectrum at high wavenumbers in azimuth direction incurred by the velocity bunching modulation, the histogram of the cut-off to mean azimuth wavenumber ratio revealed that a substantial part of the ocean swell can directly be resolved by the ERS SAR. The windsea part of the spectrum located beyond the cut-off wavenumber can also be successfully estimated through an explicit adjustment of the azimuthal cut-off wavenumber during the retrieval. Although a dependence of the azimuthal cut-off on the wind speed was clearly visible, no simple relation was found as can be expected if no fetch and wave age effects are considered.
3. A retrieval exercise using buoy spectra instead of WAM spectra as input confirmed the independence of the retrieval on the first guess. The mean spectral parameters of both the total spectra and the individual partitionings showed a good agreement. Significant differences between both retrievals were only found in the windsea part of the spectrum which can be expected as this part still contains informa-

tion from the first guess which is asymptotically truly missing in the SAR spectrum.

4. Work is under way to directly compare SWM retrievals against buoy spectra. As collocation events are rare and collocation distances should be restricted to roughly 150 km a two year data sample is needed in order to obtain satistically significant results. Furthermore, it is seeked to cover the full range of possible wave height values.

5. A statistical comparison between ERS-1 SWM retrievals and collocated WAM data computed with the operational WAM model at ECMWF was performed. Owing to their 2d spectral character the data could be sub-divided into windsea and swell constituents. The analyses revealed various features of local (windsea) and non-local (swell) character of the ocean wave field and enabled the identification of some discrepancies between the two data sets, pointing to possible shortcomings of the WAM model or the forcing wind fields which require closer investigation.

Acknowledgements: B. Hansen from ECMWF, Reading, kindly provided the WAM model data while H. Graber from RSDMAS, Miami, helped in obtaining the buoy spectra. Part of the ERS-1 FDP data were decoded by C. Melsheimer, IfM, Hamburg. We are grateful to the staff of the DKRZ for their technical assistance.

REFERENCES

Alpers, W. and K. Hasselmann, 1982: Spectral signal-to-clutter and thermal noise properties of ocean wave imaging synthetic aperture radars. *Int. J. Remote Sensing* **3**, 423-446.

Bauer, E., K. Hasselmann, I.R. Young and S. Hasselmann, 1996: Assimilation of wave data into the wave model WAM using an impulse response function. *J. Geophys. Res.* **C101** 3801-3816

Bauer, E., S. Hasselmann, P. Lionello and K. Hasselmann, 1997: Comparison of assimilation results from an optimal interpolation and the Green's function method using ERS-1 SAR wave mode spectra. in: *Proceedings of the 3rd ERS Symposium, Florence, 17 - 21 March 1997*, ESA-Publication. Also available on WWW via http://florence97.ers-symposium.org/

Brüning, C., S. Hasselmann, K. Hasselmann, S. Lehner, T. Gerling, 1995: First evaluation of ERS-1 synthetic aperture radar wave mode data. *Global Atmos. Ocean System* **2**, 61-98.

Brooker, G., 1995: ERS-1/2 UWA processing algorithm specification. Version 2.0. Reference ER-TN-ESA-GS-0342, ESTEC/NWP, Noordwijk, NL, 07/11/1995.

Chapron, B., T. Elfouhaily and V. Kerbaol, 1995: Calibration and validation of ERS Wave Mode products. *Document DRO/OS/95-02*, IFREMER, Brest (France) March 1995.

Engen, G. and H. Johnsen, 1995: SAR ocean wave inversion using image cross spectra. *IEEE Trans. Geosci. Remote Sensing* **33**, 1047-1056.

Hasselmann, K., R.K. Raney, W.J. Plant, W. Alpers, R.A. Shuchman, D.R. Lyzenga, C.L. Rufenach and M.J. Tucker, 1985: Theory of synthetic aperture radar ocean imaging. A MARSEN view. *J. Geophys. Res.* **C90**, 4659-4686.

Hasselmann, K. and S.Hasselmann [HH], 1991: On the nonlinear mapping of an ocean wave spectrum into a synthetic aperture radar image spectrum and its inversion. *J. Geophys. Res.* **C96**, 10713-10729.

Hasselmann, S., C. Brüning, K. Hasselmann and P. Heimbach [HBHH], 1996: An improved algorithm for the retrieval of ocean wave spectra from SAR image spectra. *J. Geoph. Res.* **C101**, 16615-16629.

Hasselmann, S., P. Lionello and K. Hasselmann, 1996: An optimal interpolation assimilation scheme for wave data. *J. Geoph. Res.*, in press.

Heimbach, P., S. Hasselmann and K. Hasselmann [H3], 1997: Statistical analysis and intercomparison with WAM model data of three years of global ERS-1 SAR wave Mode Spectral retrievals. Submitted to *J. Geophys. Res.*

Komen, G.J., L. Cavaleri, M. Donelan, K. Hasselmann, S. Hasselmann and P.A.E.M. Janssen, 1994: Dynamics and modelling of ocean waves. Cambridge University Press, Cambridge (UK), 1994, 560 pp.

Krogstad, H.E., O. Samset and P.W. Vachon, 1994: Generalization of the non-linear ocean-SAR transform and a simplified SAR inversion algorithm. *Atmosphere-Ocean* **32**, 61-82.

WAMDI Group (Hasselmann, K. et al.), 1988: The WAM model - a third generation ocean wave prediction model. *J. Phys. Oceanogr.* **18**, 1775-1810.